

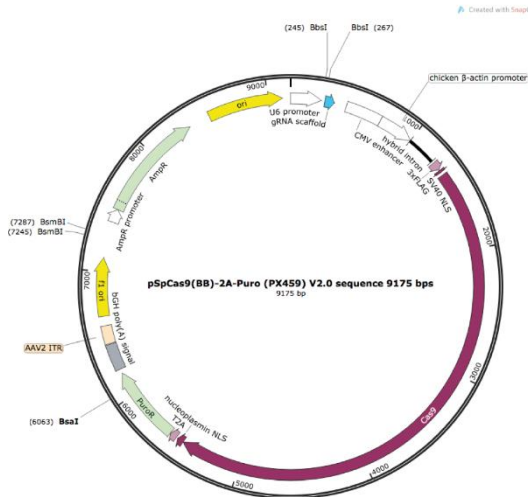
## **SUPPLEMENTARY FIGURES**

### **Dissecting the role of the NADPH Oxidase NOX4 in TGF-beta signaling in hepatocellular carcinoma**

Rut Espinosa-Sotelo<sup>a,b</sup>, Noel P. Fusté<sup>a</sup>, Irene Peñuelas-Haro<sup>a,b</sup>, Ania Alay<sup>c,d</sup>, Gabriel Pons<sup>e</sup>, Xènia Almodóvar<sup>a</sup>, Júlia Albaladejo<sup>a</sup>, Ismael Sánchez-Vera<sup>e</sup>, Ricard Bonilla-Amadeo<sup>a</sup>, Francesco Dituri<sup>f</sup>, Grazia Serino<sup>f</sup>, Emilio Ramos<sup>b,g</sup>, Teresa Serrano<sup>b,h</sup>, Mariona Calvo<sup>i</sup>, María Luz Martínez-Chantar<sup>b,j</sup>, Gianluigi Giannelli<sup>f</sup>, Esther Bertran<sup>a,b</sup>, Isabel Fabregat<sup>a,b,\*</sup>.

**A**

gRNA #1: 5'- CACCG GGTAGTGACTCTGGCCCT -3' / 5'- AAAC AGGGCCAGAGTATCACTACC C -3'  
 gRNA #2: 5'- CACCG TCACCTACCTCCACAGATGT -3' / 5'- AAAC ACATCTGGTGGAGGTAGTGA C -3'



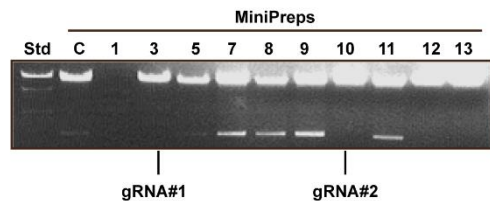
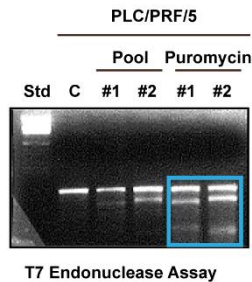
**B**

Clon 3 sequence (gRNA#1)

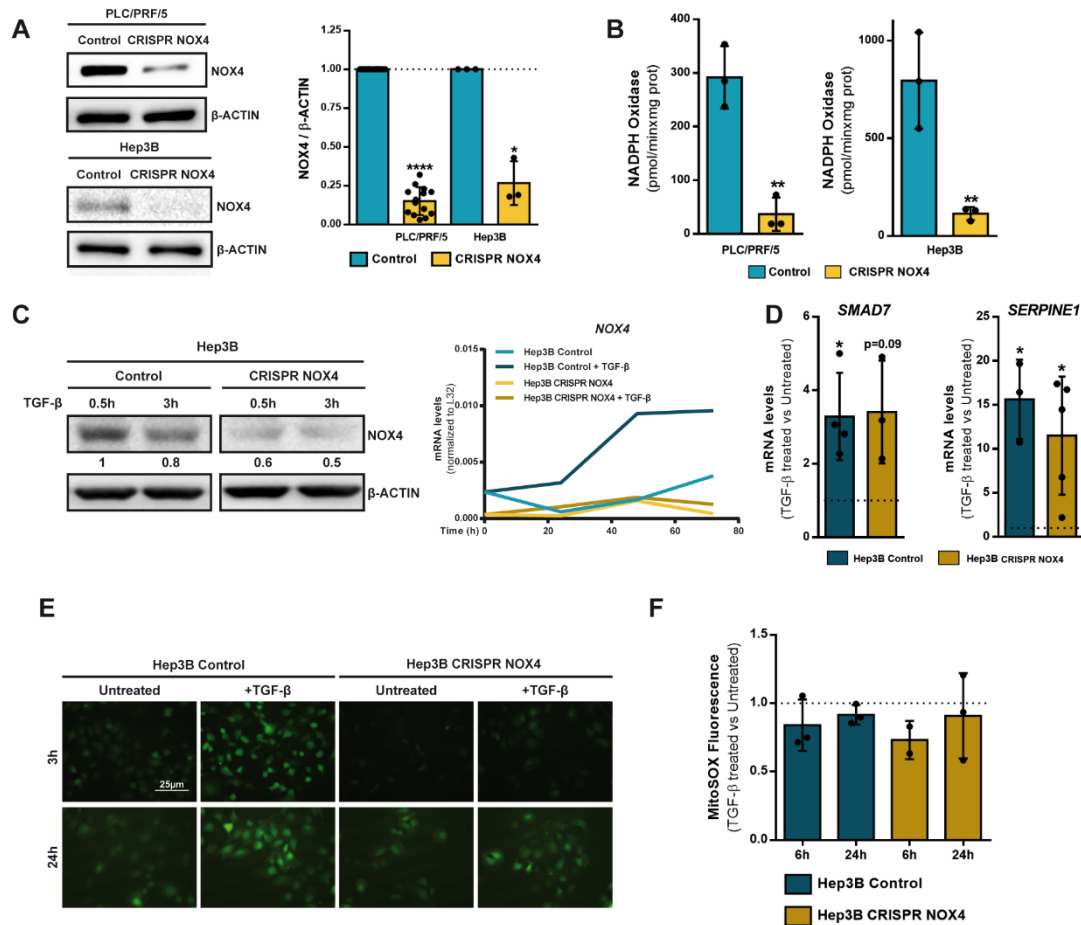
```

ATGCATCGANCAGGGCTGGTNGAGAGATAATTGGAATTAATTT
GACTGGTAAACACAAAGATATTAGTACAAAATACGTGACGTAG
AAAGTAATAATTTCTTGGGTAGTTTGCAGTTTTAAAATTATGTTT
TAAAATGGACTATCATATGCTTACCGTAACTGAAAAGTATTTCCG
ATTTCTTGGCTTTATATATCTTGTGGAAAGGACGAAACACCCGG
GTAGTGATACTCTGGCCCTGTTTTAGAGCTAGAAATAGCAAGT
TAAAATAAGGCTAGTCCGTTATCAACTTGAAAAAGTGGCACCCG
AGTCGGTGCTTTTTTGTTTTAGAGCTAGAAATAGCAAGTAAAA
TAAGGCTAGTCCGTTTTTAGCGCGTGCGCCAATCTGCAGACA
AATGGCTCTAGAGGTACCCGTTACATAACTTACGGTAAATGGC
CCGCCTGGCTGACCGCCCAACGACCCCGCCCATTTGACGTCA
ATAGTAACGCCAATAGGGACTTCCATTGACGTCAATGGGTGG
AGTATTTACGGTAAACTGCCCACTTGGCAGTACATCNGTGTAT
CANATGCCNNGTACGCCCCCNATTGACGTC
  
```

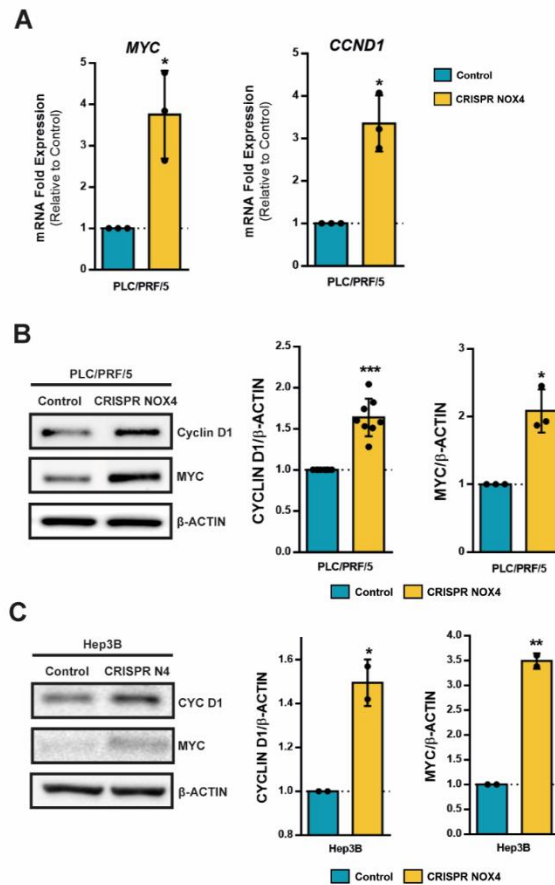
**C**



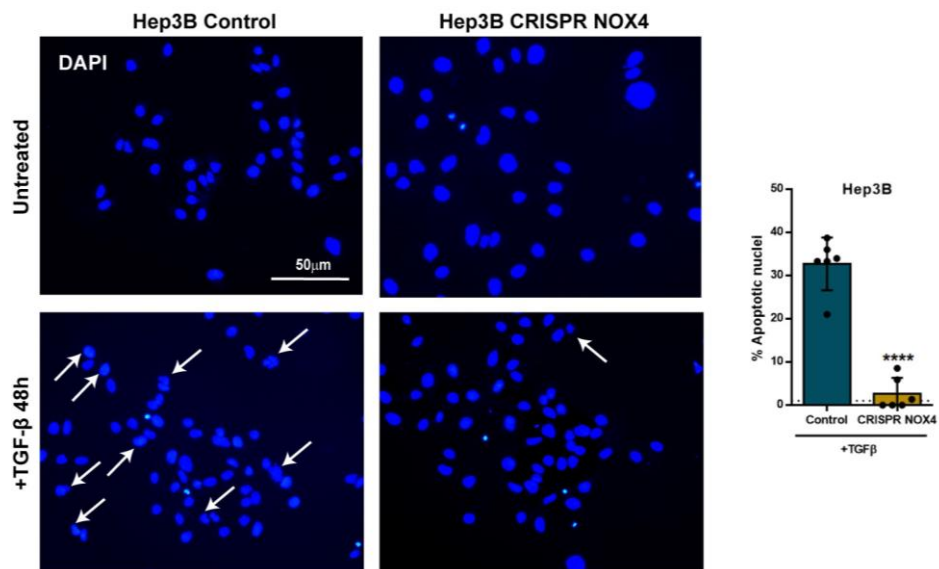
**Supplementary Figure 1. Strategy to silence NOX4 with CRISPR/Cas9 technology in HCC cells. A)** Design of RNA target guides (by bioinformatics tools) and cloning in the Cas9 vector (PX459) that contains resistance to puromycin. **B)** Selection of several clones after transformation with the different target guides: analysis of the insertion of the guide in the Cas9 vector by DNA sequencing (**top**) and restriction enzymes (**bottom**). **C)** Transfection of the HCC cell line with the different RNA target guides #1 (gRNA#1) or #2 (gRNA#2) and, after puromycin selection, T7 Endonuclease Assay to reveal if the Cas9 vector had worked correctly on the genomic DNA.



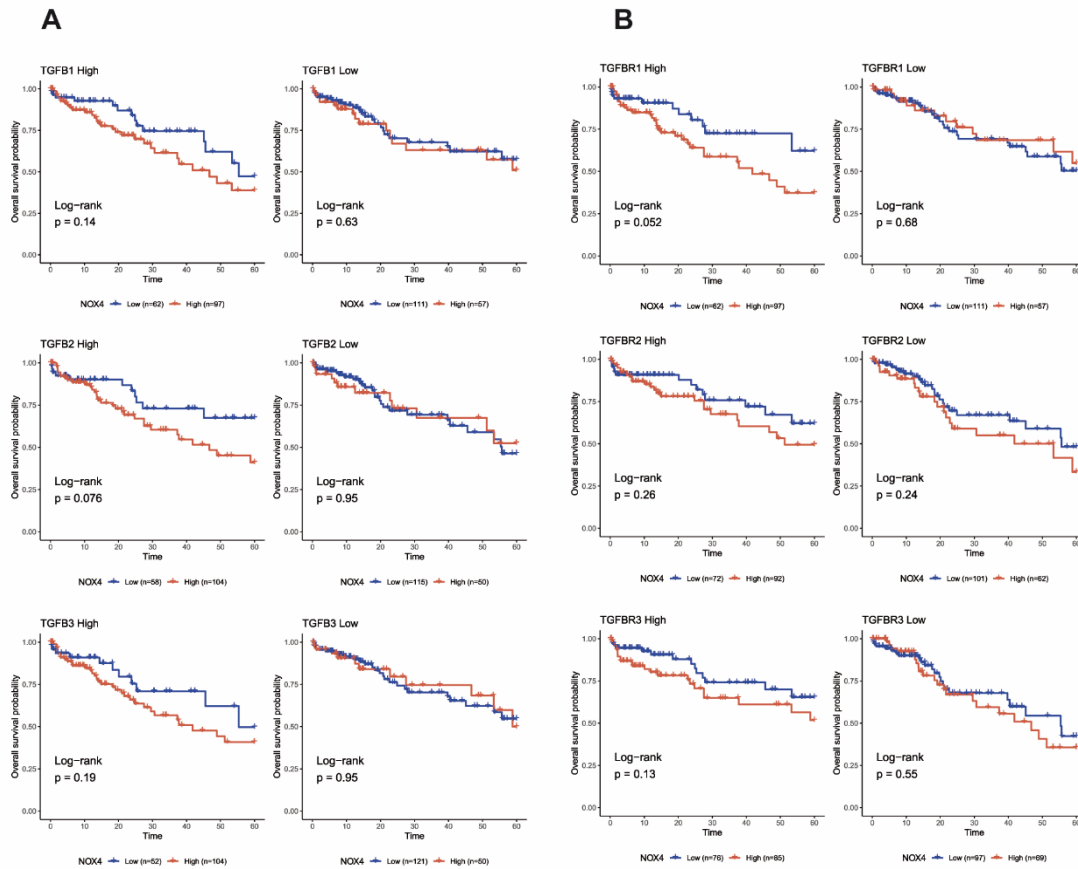
**Supplementary Figure 2. Characterization of the cellular models used in this study.** PLC/PRF/5 and Hep3B cells were stably transfected with either with a nonspecific vector (Control) or a mixture of both RNA guides #1 and #2 simultaneously (CRISPR NOX4) **A**) NOX4 protein levels analyzed by western blot.  $\beta$ -Actin was used as loading control. Representative experiment (**left**) and densitometric quantification of NOX4 levels relative to  $\beta$ -Actin (**right**). Data are Mean  $\pm$  SD,  $n \geq 3$ ). **B**) Analysis of NADPH oxidase activity, expressed as picomoles per minute per  $\mu$ g of protein. Data are Mean  $\pm$  SD ( $n = 3$ ). **C**) NOX4 expression. Protein levels analyzed by western blot after TGF- $\beta$  treatment at 0.5 and 3h.  $\beta$ -Actin was used as loading control (**left**). NOX4 mRNA expression analysed by RT-qPCR, normalized to housekeeping gene *L32*, after TGF- $\beta$  treatment at 24, 48 and 72 hours (**right**). Representative experiments are shown. **D**) *SMAD7* and *SERPINE1* mRNA expression analysed by RT-qPCR, normalized to housekeeping gene *L32*, after 48h TGF- $\beta$  treatment, represented as fold induction (TGF- $\beta$ -treated versus untreated cells). Data are mean  $\pm$  SD ( $n = 6$ ). **E**) Analysis of intracellular ROS content by  $H_2DCFDA$  after TGF- $\beta$  treatment. Scale bar, 25 $\mu$ m. **F**) Mitochondrial  $O_2^{\cdot -}$  analyzed fluorometrically using MitSOX<sup>TM</sup>. Results are expressed as relative to each control. Data are mean  $\pm$  SD ( $n \geq 3$ ). Statistical analysis, where indicated: \* $p < 0.05$  \*\* $p < 0.01$ , \*\*\* $p < 0.001$ , comparing CRISPR NOX4 cells versus CRISPR Control in A and B and TGF- $\beta$ -treated versus untreated condition in D.



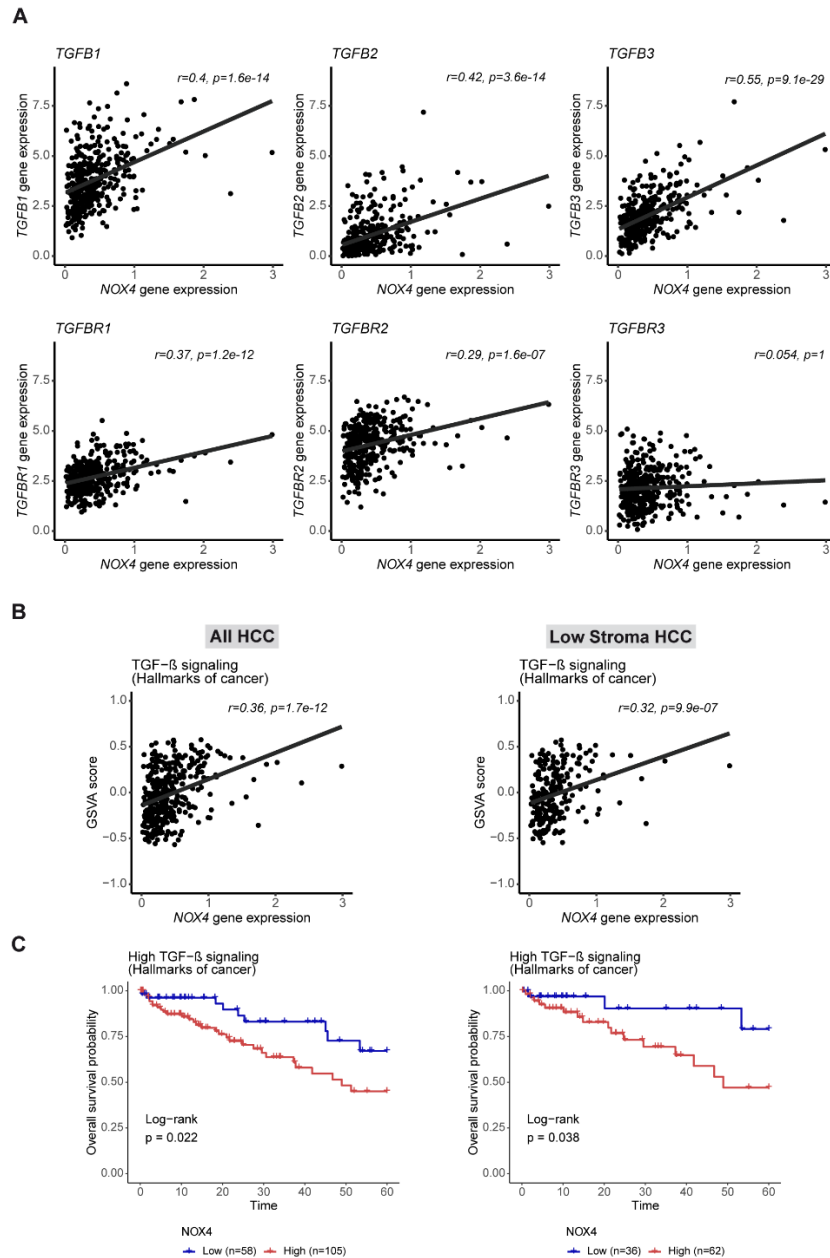
**Supplementary Figure 3. *MYC* and *CCND1* (Cyclin D1) expression levels in HCC (Control and CRISPR NOX4) cells. A) *MYC* and *CCND1* mRNA expression analysed by RT-qPCR, normalized to housekeeping gene *L32*, in PLC/PRF/5 cells. B-C) C-MYC and Cyclin D1 protein levels analyzed by Western blot in both PLC/PRF/5 (B) and Hep3B (C) cells.  $\beta$ -Actin was used as loading control. Representative experiment (left) and densitometric quantification of protein levels expressed as relative to  $\beta$ -Actin (right). Data are mean  $\pm$  SD (n $\geq$ 3). \*p<0.05 \*\*p<0.01, \*\*\*p<0.001.**



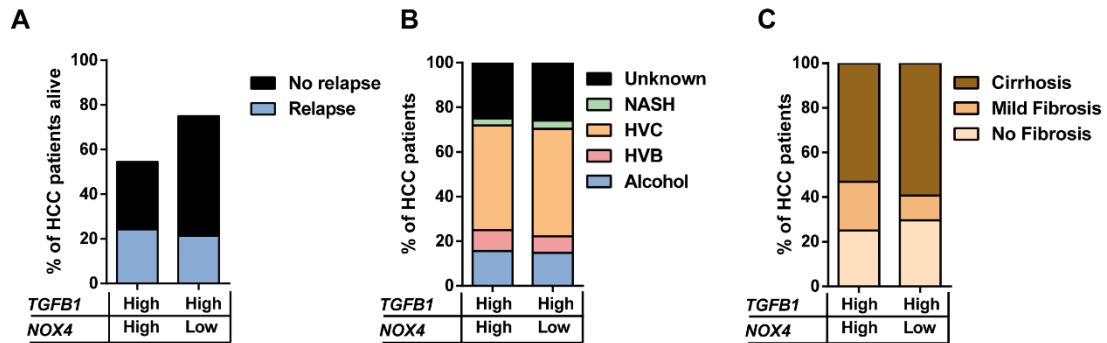
**Supplementary Figure 4. Role of NOX4 on TGF- $\beta$ -induced apoptosis.** Analysis of fragmented nuclei (arrows) after DAPI (blue) staining in cells untreated or treated during 48 h with TGF- $\beta$ . Representative images (**left**) and quantitative analysis (using ImageJ software), each dot representing one field (**right**).



**Supplementary Figure 5. Kaplan-Meier curve for overall survival (OS) probability for *NOX4*-low versus *NOX4*-high HCC patients, stratified by TGF- $\beta$  ligands and receptors expression levels. Data from TCGA-LIHC public data base (n=327). **A**) TGF- $\beta$  ligands: OS when *TGFB1*, *TGFB2* or *TGFB3* are high (**left**) or low (**right**). **B**) TGF- $\beta$  receptors: OS when *TGFBR1*, *TGFBR2* or *TGFBR3* are high (**left**) or low (**right**). Genes are categorized using the median, and p-values are derived from a log-rank test.**

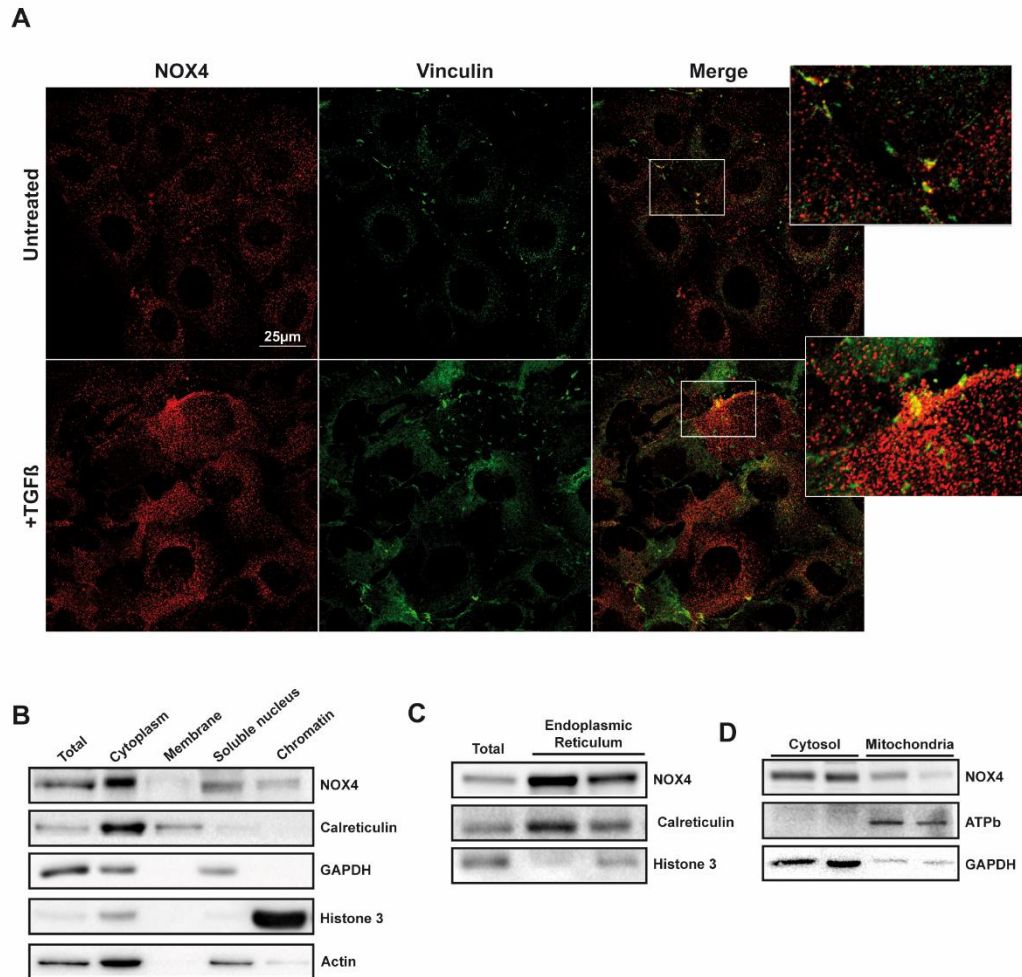


**Supplementary Figure 6. In silico analysis of the correlation of NOX4 expression and genes encoding TGF- $\beta$  ligands, receptors, and a TGF- $\beta$ -signalling gene signature (Hallmarks of Cancer) (see Table 3). Data from TCGA-LIHC public data base (n=327). **A**) Pearson correlation analysis between NOX4 gene expression and TGFB1, TGFB2 or TGFB3 (top) or TGFBR1, TGFBR2 or TGFBR3 (bottom). **B**) Pearson correlation analysis between TGF- $\beta$  signalling (quantified using Gene Set Variation Analysis (GSVA) score) and NOX4 gene expression. Analysis done with all the HCC samples (left) or those with low stromal content (right). **C**) Kaplan-Meier curve for overall survival probability for NOX4-low versus NOX4-high patients when “TGF- $\beta$ -signalling Hallmarks of Cancer” gene signature is high (above the median GSVA score). NOX4 is categorized using the median, and log-rank test is used to assess statistical differences. Analysis done with all the HCC samples (left) or those with low stromal content (right).**

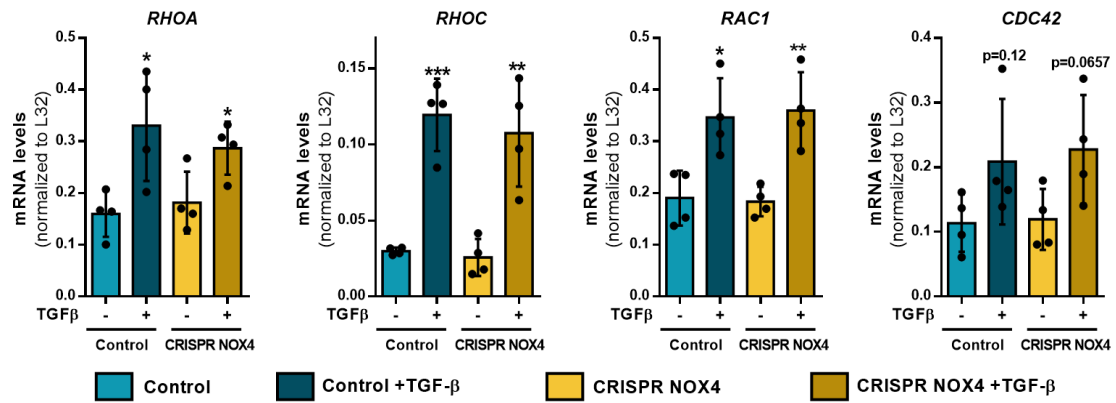


**Supplementary Figure 7. Impact of the expression of NOX4 on relapse, fibrosis and aetiology in HCC patients with high expression of *TGFB1*.** Analysis performed in alive patients at the time of analysis. **A)** Percentage of patients that suffered relapse versus those that did not. **B)** Percentage of HCC patients with different aetiologies: Alcohol, HVB, HVC, NASH or Unknown origin. **C)** Percentage of HCC patients presenting fibrosis, mild fibrosis or cirrhosis.

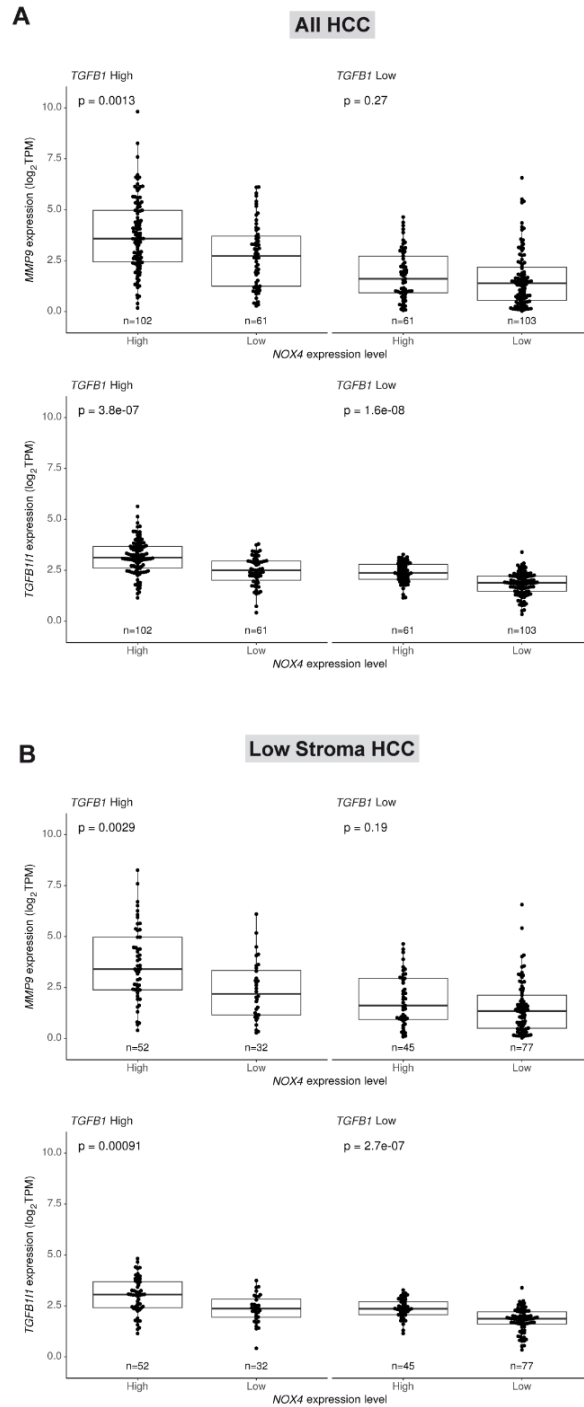




**Supplementary Figure 8. NOX4 protein localization in different cellular compartments.** Analysis made in Hep3B Control cells. **A)** Immunofluorescence of NOX4 (red) and Vinculin (green) in cells either untreated or treated during 48h with TGF- $\beta$ . Representative images are shown. Scale bar, 25 $\mu$ m. **B)** NOX4 protein levels analyzed by western blot in different subcellular fractions of untreated PLC/PRF/5 cells, extracted as described in the Material and Methods section. **C)** Similar analysis in total or Endoplasmic Reticulum (ER) fractions and **D)** in Cytosol and Mitochondria fractions. Marker proteins to follow fractionation were: Calreticulin for endoplasmic reticulum (ER), GAPDH for cytosolic compartment, ATPb for mitochondria and Histone 3 for chromatin. Images representative of at least 3 independent experiments.



**Supplementary Figure 9. NOX4 silencing in HCC Hep3B cells do not affect the response to 48h TGF-β treatment in terms of RhoGTPases family gene expression. *RHOA*, *RHOC*, *RAC1* and *CDC42* mRNA expression analysed by RT-qPCR, normalized to housekeeping gene *L32*, after TGF-β treatment at 48 hours. Data are Mean ± SD (n=4). \*p<0.05 \*\*p<0.01, \*\*\*p<0.001.**



**Supplementary Figure 10. In silico analysis of the expression of *MMP9* and *TGFB111*.** **A)** Boxplot of *MMP9* (**top**) or *TGFB111* (**bottom**) gene expression for *NOX4*-low versus *NOX4*-high patients when *TGFB1* expression is low or high. Analysis done with all the HCC samples. **B)** Boxplot of *MMP9* (**top**) or *TGFB111* (**bottom**) gene expression for *NOX4*-low versus *NOX4*-high patients when *TGFB1* expression is low or high. Analysis done with low stromal content samples. Data from TCGA-LIHC public data base (n=327). P-values from a Mann-Whitney U test, adjusted for multiple testing.